Ab Initio Size-Consistent Calculations of Effective Exchange Interactions in Mesoscopic Magnetic Clusters Composed of Triplet Methylenes and Quartet Nitrogen Atoms

Takashi Kawakami, Syusuke Yamanaka, Yu Takano, Yasunori Yoshioka, and Kizashi Yamaguchi*

Department of Chemistry, Graduate School of Science, Osaka University, Toyonaka, Osaka 560

(Received April 2, 1998)

The electronic structures of linear magnetic clusters composed of eleven triplet methylenes, eleven quartet nitrogen atoms, and five triplet methylenes plus six quartet nitrogen atoms were investigated by the unrestricted Hartree–Fock (UHF), post UHF and their spin-projected wavefunctions in combination with the Heisenberg model. The effective exchange integrals (J_{ab}) in the Heisenberg model were calculated by the difference between the total energies of the highest spin (HS) and lowest spin (LS) UHF-based wavefunctions of the clusters. The J_{ab} values by the UHF-based and spin-polarized DFT methods were compared with those of the SO-Cl, MRSDCI, CASSCF, CASPT2, and MRMP2 calculations in the case of small linear clusters, such as a triplet methylene dimer. The spin-polarized density functional (BLYP and B3LYP) calculations followed by the size-consistent spin projection were carried out for dimer, trimer, and clusters with eleven magnetic sites to obtain the J_{ab} values, since the DFT methods were heavily utilized in solid state physics. It was found that all of the methods, except for DFT, provide similar J_{ab} values in the magnetic region of the dimer, where the interatomic distance is longer than 3.0 Å. However, the spin crossover from the LS state to the HS state occurs at a larger distance in the cases of MRSDCI and MRMP2. The spin projection for LS spin-polarized wavefunctions becomes less important in the case of long linear clusters, such as $(CH_2)_{11}$. The DFT results are generally biased to stabilize the low-spin states. The implications of the calculated results are discussed in relation to the molecular magnetisms in mesoscopic molecular aggregates.

Molecule-based magnetic materials have received continuous experimental and theoretical interest. As is well known, the electronic structures and thermodynamic properties of low-dimensional magnetic clusters, chains, and sheets are classic and fundamental problems, and many theoretical studies have already been carried out.[1)] During of the past decade these systems have also been extensively investigated in relation to the magnetic behaviors of transition metal complexes,[1)] as well as the so-called high-T_c superconductivity of copper oxides and related systems.[2)] Possible organic analogs to copper oxides have also received both theoretical and experimental interest, and several interesting results have been recently reported.[1,3)] However, theoretical studies on inorganic and organic systems with strong electronic correlations are usually based on the effective model Hamiltonians derived from experimental results. First-principle calculations have been rather limited, though many experimental results have been reported.[1,2)]

From the recent discovery of magnetic long-range orders in organic solids,[1)] it can be seen that the transition temperatures (T_c) for ferromagnets are very low, and the working hypotheses for raising T_c are hardly derived only from the experimental results. Therefore, theoretical studies of organic radical solids are crucial and important for the molecular design of high-T_c organic ferromagnets and new magnetic materials. Such efforts have been already initiated by several groups.[1,4)] Previously, we also examined dimer to pentamer in order to elucidate the overlap and orientation principles for spin alignments and to calculate the effective exchange interactions (J_{ab}) in the Heisenberg model.[5)] The organic ferromagnetism of *para*-nitrophenyl nitronylnitroxide (*p*-NPNN) was successfully explained by using the calculated effective exchange integrals.[5)]

Very recently, magnetic clusters with short-range orders have attracted great interest from the view point of macroscopic quantum tunnelling (MQT) and related phenomena, such as a single-molecule magnet. Several experimental studies have been carried out for elucidating both the static and dynamic behaviors in the species.[1,2)] Judging from the recent experiments,[1)] nano-scale magnetic clusters are not only interesting from the viewpoint of fundamental chemistry, but are also important concerning applications to molecular devices. Since the magnetic clusters which presently concern us are rather large, the size-consistency problem becomes serious in any theoretical treatment of the species. Ab initio size-consistent calculations of the J_{ab} values are thus one of current theoretical problems.

In this paper we first summarize the theoretical aspects in Section 1 in relation to molecular magnetism. Both spin-restricted and unrestricted post Hartree–Fock methods are briefly reviewed in relation to the first-principle computation of effective exchange integrals. The J_{ab} values calculated by the UHF-based methods were compared with those previously estimated by SO-CI, MRSDCI, CASSCF, CASPT2,

and MRMP2 calculations[6] in the case of small linear clusters such, as the triplet methylene dimer. However, the J_{ab} values of the clusters in the mesoscopic region have not yet been thoroughly studied. We discuss the electronic structures of linear magnetic clusters comprising eleven triplet methylene, eleven quartet nitrogen atoms, and five triplet methylenes plus six quartet nitrogen atoms in Sections 2 and 3. Spin-polarized density functional (BLYP and B3LYP) calculations followed by a size-consistent spin projection have also been carried out for comparisons with these methods, since the DFT methods are heavily used in the solids state physics. The effective exchange integrals for these species in the Heisenberg model were calculated based on the difference of the total energies between the lowest-spin (LS) and highest-spin (HS) states. Both UMP2 and DFT computations were carried out for clusters with eleven magnetic sites, since the latter method is now heavily used for metal clusters and large clusters. The implications of the calculated results are discussed in relation to the molecular magnetism in mesoscopic molecular agregates.

1. Theoretical Backgrounds

1. 1. UHF Solutions for Polyradicals. We first summarize theoretical aspects which are necessary for ab initio calculations of the J_{ab} values.[1] Let us consider the potential curve of linear clusters with a variation of the interatomic distance, as illustrated in Fig. 1. It is often classified into three regions.[7] Region I is a nonmagnetic or weak correlation region, which is characterized by strong orbital interactions and the formation of strong covalent bonds. Region III is regarded as being a magnetic region where component radicals exhibit weak intermolecular interactions. Region II is characterized as a transition region from the nonmagnetic Region I to the magnetic Region III. The ab initio restricted Hartree–Fock (RHF) molecular orbital (MO) and closed-shell DFT methods[8,9] have been utilized to elucidate the electronic structures of closed-shell linear clusters in Region I. However, the intrinsic deficiency of the RHF MO and closed-shell DFT methods is that they can not describe the dissociation process of a covalent bond from Region I to III, even in a qualitative sense.[7] One approach to this problem within the Hartree–Fock (HF) MO and DFT frameworks is to use the unrestricted HF (UHF) and spin-polarized DFT theories.[10] The bifurcation of the RHF (DFT) close-shell MOs into the UHF different-orbitals-for-different-spins (DODS) or spin-polarized DFT MOs occurs at the triplet (T) instability threshold where the lowest eigenvalue of the T-instability matrix is zero ($\lambda_0 = 0$).[11—14] This means chemically that the molecule under consideration has a singlet biradical or polyradical character[15] if the interatomic distances exceed the instability thresholds.

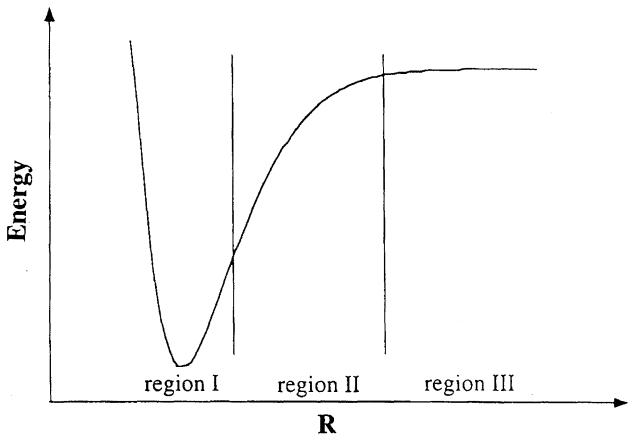

Fig. 1. Schematic illustrations of potential curve for the lowest-spin (LS) ground state of one-dimension cluster with variation of interatomic distance *R*. Regions I is a nonmagnetic region, III is a magnetic regin, and II is a intermediate region.

The UHF MO and spin-polarized DFT methods offer qualitatively correct orbital pictures and an orbital correlation diagram for the dissociation of a covalent bond, being applicable to biradical and polyradical species.[15] However, the UHF-based and spin-polarized DFT wavefunctions for singlet biradicals and low-spin species suffer from spin contaminations arising from high-spin states,[10] leading to spin-projection procedure.[16—18] Previously, we examined several aspects of the spin projections in the case of dimers of triplet methylenes.

The dynamical correlation correction for UHF wavefunctions are usually taken into account by the Möller–Plesset (MP) perturbation[19] and coupled-cluster (CC) theories.[20] However, the spin-contamination terms cannot be removed by the MP and CC corrections. The projected UMP scheme[17,21] is in principle feasible for any polyradicals, but causes a small energy unbalance between spin multiplets in the case of an approximated scheme implemented in the GAUSSIAN 94 program package.[22] On the other hand, the Löwdin-type spin projection[21] for the UHF CC (UCC) wavefunctions has not yet been developed. Here, we use an approximate but size-consistent spin projection (AP) scheme for UMP and UCC, and DFT solutions presented previously.[5,16]

However, the size-dependency of the J_{ab} values has not yet been thoroughly investigated.[5,6] Experimentally, superparamagnetism and short-range orders have been observed if magnetic cluster sizes exceed a certain limit.[1,2] This in turn means that the spin-projection effect for broken-symmetry UHF and DFT should be more or less reduced for large magnetic clusters. In fact, such a tendency is confirmed later.

1. 2. UNO CAS CI and UNO CASSCF for Polyradicals. In order to include all spin coupling terms, the full configuration interaction (FCI) by the use of all natural orbitals related to the dissociation processes shown in Fig. 1 is one of the practical approaches. As an extension of the UHF MO-theoretical approach to unstable molecules, we have investigated the utility of approximate natural orbitals[23] and their occupation numbers determined by UHF calculations for selections of active orbitals of the complete active space (CAS) configuration (CI) or the multi-reference (MR) CI[24] and for the rapid convergence of MCSCF calculations.[25] Judging from the magnitude of the occupation numbers,

UNOs are classified into (1) core, (2) active, and (3) secondary groups.[26] The full CI (FCI) is performed within active UNOs as

$$\Phi \text{ (UNO CASCI or UNO CASSCF)} = \Sigma C_i \Phi_i, \quad (1)$$

where Φ_i are all of the configurations constructed of active UHF NO (UNO) and C_i are their expansion coefficients. The size of CAS is usually taken to be sufficient for descriptions of the highest-spin (HS) and lowest-spin (LS) states of polyradicals. When the UNO and CASCI vector are utilized as trial orbitals[25] for the more refined CASSCF calculations[27] of the state under consideration, the procedure is often called a specific UNO CASSCF.[25,28,29] Dynamical correlation corrections can be incorporated by the second-order perturbation (PT2) method based on the CASSCF wavefunctions. This CASPT2 approach[30,31] is efficient for smaller polyradicals, but cannot be applicable to larger systems, since CAS often becomes over 15 orbitals. Therefore, more practical methods are necessary for ab initio calculations of the J_{ab} values[1] for the nanoscale magnetic clusters of our present concern.

1. 3. Approximate Spin Projections for UHF and DFT. The UNO CASSCF calculations give by Eq. 1 are desirable for depicting potential curves in all regions shown in Fig. 1. Such treatments are, however, very difficult for magnetic clusters, since the number of CAS active orbitals exceeds the current limit (15 orbitals at the present state). On the other hand, spin projection is easy for the Heisenberg (HB) clusters in Region III, since UHF and spin-polarized DFT orbitals for radical sites are essentially orthogonal. Since the total energies of the HS and LS UHF (or DFT) solutions correspond to those of the HB models, respectively, the energy gap can be used to estimate the effective exchange integrals (J_{ab})[5] as

$$J_{ab}(Z) = [{}^{HS}E(Z) - {}^{LS}E(Z)]/\Delta(ZI), \quad (2)$$

where,

$$\Delta\,(ZI) = 4\,(N-1)\,S_a S_b, \quad (3)$$

and Z = UHF or DFT, and N is the number of spin sites in clusters under consideration. S_a and S_b are the sizes of spin at sites a and b, as illustrated in Fig. 2. The energy gain by the spin projection can be estimated by Eqs. 2 and 3, since J_{ab} (Z) is determined even for larger systems. If the electron correlation is taken into account under the UHF approximation, the effective exchange integrals by UHF in Eq. 2 are replaced by that of UHF-X (X = MP, CCSD, CCSD-(T)).

$$J_{ab}(\text{UHF-X}) = [{}^{HS}E(\text{UHF-X}) - {}^{LS}E(\text{UHF-X})]/\Delta(ZI). \quad (4)$$

On the other hand, the spin projection of the UHF-X wavefunctions in Region II is a difficult task, since the orbital overlaps between radical orbitals are significantly large. The Löwdin-type spin-projection scheme[17] is utilized for this purpose. However, it often provides incorrect J_{ab} values because of the introduced approximations.[6] Alternately, approximate spin projections[5,6] are feasible for UHF-based and spin-polarized DFT methods to calculate potential curves for dissociations from Region I to Region III. To this end, we have considered an approximate but size-consistent spin-projection procedure, where the denominator in Eq. 2 is modified so as to reproduce the extremal values of total spin angular momentum in Regions I and III as[5]

$$\Delta(ZII) = {}^{HS}\langle S^2\rangle(Z) - {}^{LS}\langle S^2\rangle(Z) - S_a g(N)[{}^{LS}\langle S^2\rangle(Z) - S_r(S_r+1)], \quad (5)$$

where $g(N) = (N-2)^2/N$ ($N > 2$ and even numbers), (6a)

or $= (N-3)$ ($N > 3$ and odd numbers), (6b)

and Z = UMP, UCC or DFT, and S_r denotes the exact spin angular momentum for the clusters under discussion:

$$S_r = n\,(S_a - S_b) \quad (N = 2n), \quad (6c)$$

or $$S_r = n\,(S_a - S_b) + S_a \quad (N = 2n+1). \quad (6d)$$

The effective exchange integral by the approximate spin-projected (AP-) UMP, UCC, and DFT methods are, therefore, given by[32—35]

$$J(\text{AP-Z}) = [{}^{HS}E(Z) - {}^{LS}E(Z)]/\Delta(ZII). \quad (7)$$

The J_{ab}(AP-Z) value almost reduces to that of Eq. 2 in magnetic Region III, whereas it becomes a theoretical parameter for the spin projection in the intermediate (II) and strong overlap (I) regions, where the spin-contamination effects in UHF and spin-polarized DFT wavefunctions are more or less decreased.

The potential curves by the UMP method often show humps[16—18] arising from the spin contaminations. The J_{ab}(AP-Z) values in Eq. 7 can be used to improve the shapes of the potential curves Z, as illustrated in Fig. 3.[35] The total energies by AP-Z are given by[5]

$${}^{LS}E(\text{AP-Z}) = {}^{LS}E(Z) + J_{ab}(\text{AP-Z})[{}^{LS}\langle S^2\rangle(Z) - S_r(S_r+1)] \times [1 - h(N)], \quad (8)$$

where $h(N) = (N-2)^2/N^2$ ($N > 2$ and even numbers), (9a)

or $= (N-3)/(N+1)$ ($N > 3$ and odd numbers). (9b)

The AP-Z energy reduces to that of RHF-X or ORHF-X (X = MP, CC) in Region I, since the second term in Eq. 8 disappears, whereas it becomes equivalent to the projected UHF-X energy by Eq. 2 in Region III. As previously shown,[35,36] the AP-Z potential curves are good approximations to those of UNO CASSCF PT2 (CASPT2) in the case of small hydrogen clusters. The energy correction by spin projection should be normalized by the size of the cluster (N) in order to appropriately estimate the projection effect for large N.

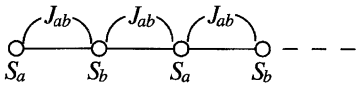

Fig. 2. One-dimension magnetic cluster with sizes of spins, S_a and S_b, at sites a and b, and also a uniform effective exchange integral (J_{ab}) between sites a and b.

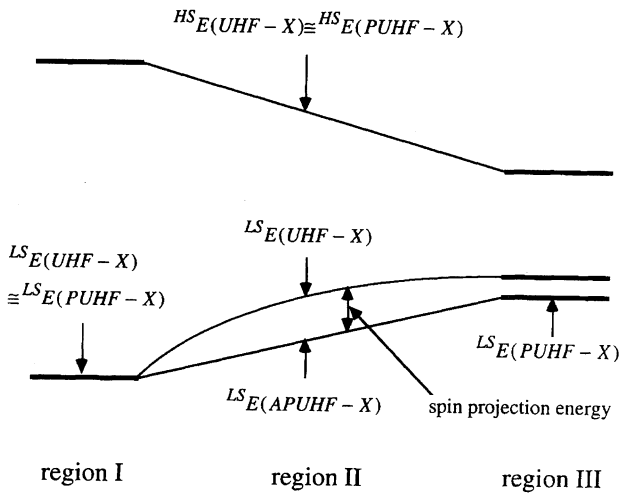

Fig. 3. Schematic illustrations of the potential curves of spin-unprojected and -projected post UHF solutions (UHF-X) for mesoscopic clusters with N-magnetic sited.

$$\Delta E(\text{AP-Z}) = [{}^{\text{LS}}E(\text{AP-Z}) - {}^{\text{LS}}E(\text{Z})]/N \tag{10}$$

$$= J_{\text{ab}}(\text{AP-Z})[{}^{\text{LS}}< S^2 > (\text{Z}) - S_{\text{r}}(S_{\text{r}}+1)][1-h(N)]/N \tag{11}$$

Figure 4 shows variations in the size correction term ($1-h(N)$) with the total spin site number (N). Since ${}^{\text{LS}}<S^2>(\text{Z})$ is approximately proportional to N, the projection effect of Eq. 11 approaches zero if N becomes larger. In fact, for large N,

$$\Delta E(\text{AP-Z}) \approx 4\, J_{\text{ab}}(\text{AP-Z})/N. \tag{12}$$

Therefore, the spin-projection correction for the LS state decreases along with an increase in the cluster size (N) and the energy correction by the spin projection is negligible if the site number N exceeds a certain limit.

1. 4. Orbital Average Effective Exchange Integrals. The effective exchange integrals (J_{ab}) can be extended to radical sites with more than one electron, and are generally described by an orbital average form given as

$$J_{\text{ab}} = \frac{1}{m \times n}\sum_{i=1}^{m}\sum_{j=1}^{n} J_{ij} \tag{13}$$

where m and n denote the number of unpaired spins at radical sites a and b. Therefore, the sign of J_{ab} is determined by the detailed balance of the orbital components (J_{ij}).

It was previously[37,38] demonstrated that the treatment of the orbital average effective exchange integrals is applicable for describing the effective exchange interaction of clusters of transition metals, such as Mo(II)[39] and Cr(II).[40] The electronic structures of Mn(III)–Mn(IV) pair[41] and [Fe_mS_n] systems,[37,41] which have different spin sizes at the nearest radical sites, are also well presented by the orbital average effective exchange integrals. The clusters comprising triplet methylene examined in this paper have two radical orbitals on the carbon atoms, while the quartet nitrogen atom has three radical orbitals. The clusters of triplet methylene are typical examples of organic systems possessing more than one electron at radical sites. The clusters comprising triplet methylene plus the quartet nitrogen atoms also correspond to a system with different spin size at radical sites.

1. 5. Shapes of Potential Energy Curves. The effective exchange integrals (J_{ab}) in the Heisenberg model were calculated by the difference between the total energies of the highest spin (HS) and lowest spin (LS) states of the clusters as shown in Eqs. 2, 4, and 7. Estimations of the total energies of the lowest spin state by an approximated spin-projected wave function are given by Eq. 8. Profiles of their energies are schematically illustrated in Fig. 3. It is interesting to draw the potential energy curves of HS, LS, and approximated spin-projected (AP-) LS states of real clusters examined in this paper in order to elucidate the behaviors of the potential energies with size effects of clusters before the J_{ab} values are discussed.

As examples, drawn in Fig. 5 are the potential energy curves of the face-to-face (parallel conformation) dimer of triplete methylenes and a cluster comprising eleven triplet methylenes, as illustrated in Fig. 6B, at the level of UMP2. The UMP2 method for the face-to-face dimer of triplet methylene gives potential energies curves similar to those previously obtained by the CASPT2(D) method,[6b] suggesting that the APUMP2 method can reproduce effective exchange integrals obtained by CASPT2(D) in a semi-quantitative manner. It is applicable to larger clusters which have antiferromagnetic or ferromagnetic spin couplings of high-spin molecules.

It can be seen from Fig. 5 that the approximated spin-projected states of the LS state for both dimer and clusters of eleven methylenes are lower in energy than the LS state over the entire regions of the interatomic distances. These behaviors obviously indicate that the clusters examined here at least do not belong to region I shown in Figs. 1 and 3. From Fig. 5, the energy lowerings from the LS state to the AP-LS state for both the dimer and eleven-cluster are comparable to each other with values nearly equal to 0.005 au. However, according to the energy correction defined by Eq. 10, the projection effect of the LS state in the cluster of $(CH_2)_{11}$ is

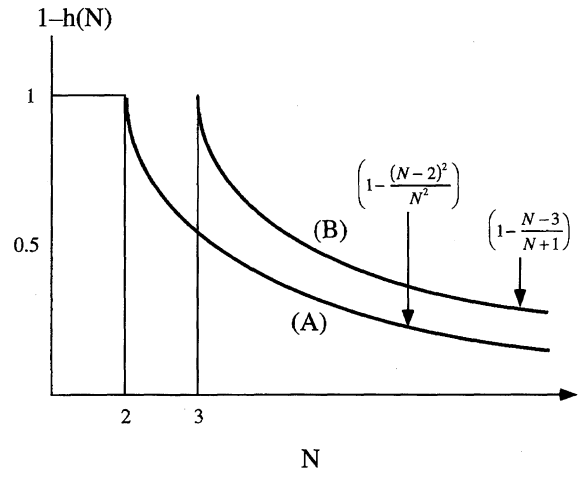

Fig. 4. Variations of the size-correction term $(1-h(N))$ shown in Eqs. 8 and 9 of text with the total site number N.

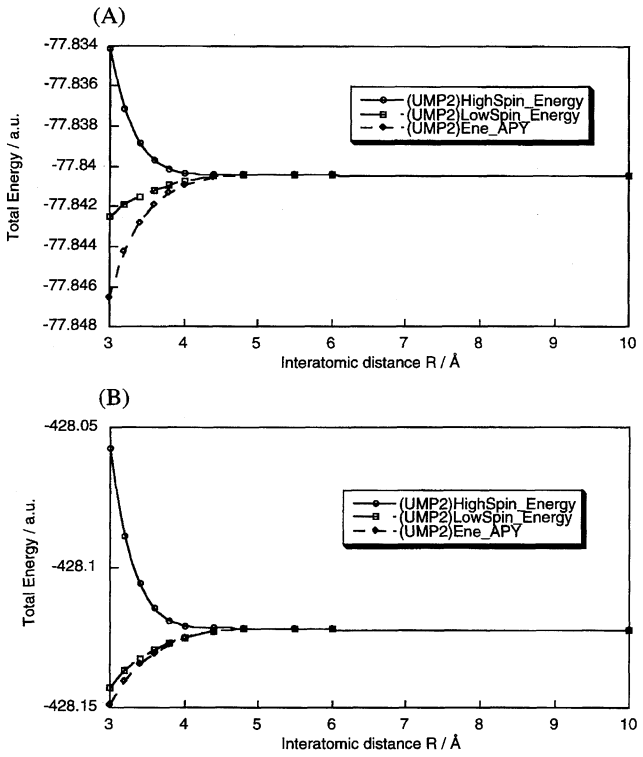

Fig. 5. Potential energy curves of highest-spin (HS), lowest-spin (LS) and the approximated spin-projected (AP-) LS states of (A) dimer of triplet methylenes and (B) cluster composed of eleven triplet methylene estimated at level of UMP2.

apparently smaller than those in the dimer of CH_2, indicating that the approximated spin-projection is less important for a larger size of clusters.

2. MO Calculations of J_{ab} Values

2. 1. Linear Clusters of Triplet Methylenes. Let us first consider the face-to-face (parallel conformation) dimer, trimer, and cluster (N=11) of triplet methylenes, as illustrated in Figs. 6A and 6B. The effective exchange interactions between triplet methylenes in the dimer (**1**) were calculated from Eqs. 2 and 7 using the total energies of the lowest-spin (LS) singlet and the highest-spin (HS) quintet states of **1** by the UHF/6-31G* method. Table 1 summarizes the calculated results. The calculated J_{ab}values were negative (antiferromagnetic) in sign over the entire intermolecular interaction region (3.0 Å$<R<$10 Å) examined here. The magnitude of J_{ab}(UHF) by Eq. 2 and J_{ab}(APUHF) by Eq. 7 are quite similar, showing that the orbital overlaps between the magnetic orbitals are very small in the region.[5,6] The J_{ab}(APUHF) values are also close to the corresponding J_{ab} values by CASSCF, which utilizes the four active orbitals and four active electrons {4,4}.[6] This indicates that both APUHF and UNO CASSCF involve only the so-called nondynamical correlation within the {4,4} space.[26] It is noteworthy that a larger CAS space than {4,4} is necessary for the latter approach to include dynamical correlation corrections.

Next, we examined the trimer (**2**) of triplet methylenes, as illustrated in Fig. 6A. Only the nearest-neighbor J_{ab} values

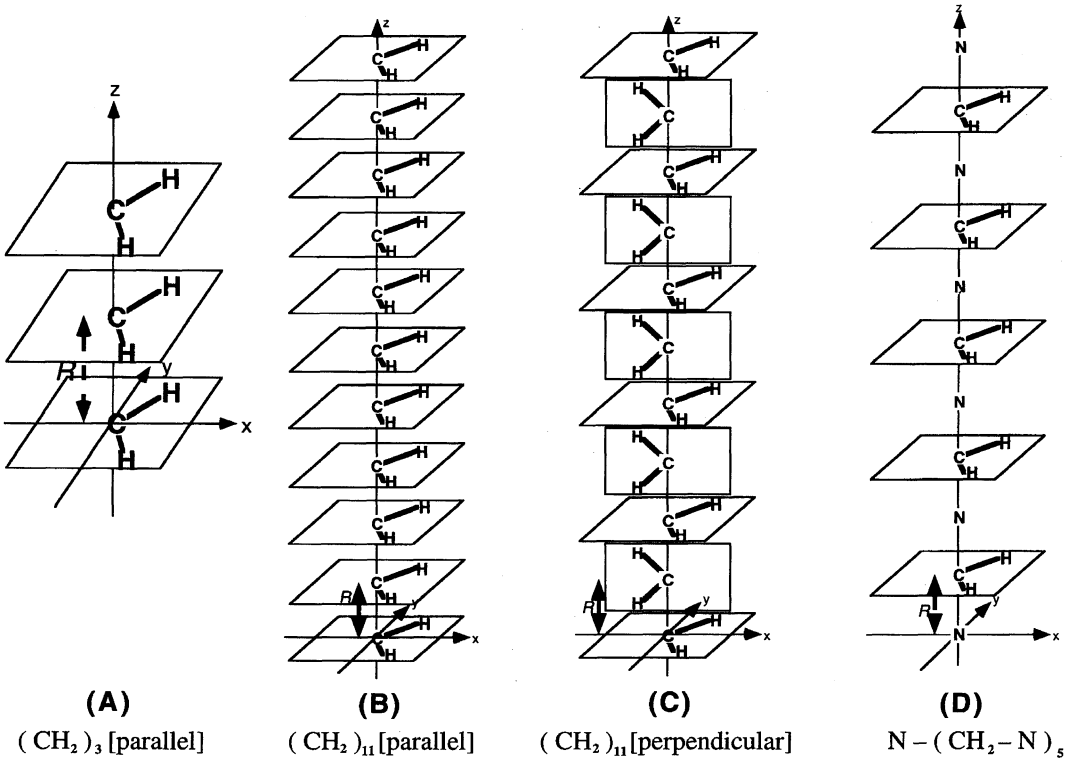

(A) $(CH_2)_3$ [parallel] (B) $(CH_2)_{11}$ [parallel] (C) $(CH_2)_{11}$ [perpendicular] (D) $N-(CH_2-N)_5$

Fig. 6. Schematic illustrations of liner clusters composed of triplet methylenes and quartet nitrogen atoms; (A) trimer of triplet methylenes in the face-to-face stacking, (B) eleven triplet methylenes in the face-to-face stacking, (C) eleven triplet methylenes in the perpendicular stacking, (D) five triplet methylenes and six quartet nitrogen atoms.

Table 1. Effective Exchange Integrals J_{ab} (cm^{-1}) of Clusters Composed of Triplet Methylene

R	$(CH_2)_2$[||]$^{a)}$				$(CH_2)_3$[||]$^{a)}$		$(CH_2)_{11}$[||]$^{a)}$		$(CH_2)_{11}$[⊥]$^{b)}$	
Å	UHF$^{c,d)}$	APUHF$^{c,d)}$	CASSCF$^{c)}$		UHF$^{c,d)}$	APUHF$^{c,d)}$	UHF$^{e)}$	APUHF$^{e)}$	UHF$^{e)}$	APUHF$^{e)}$
3.0	−401.2	(−390.8)	−396.6	(−386.5)	−411.7	−405.7	(−393.3)	−400.7	(−393.3)	−395.4	−371.6	141.7	144.5
3.2	−228.6	(−220.7)	−227.1	(−219.3)	−233.1	−230.2	(−221.4)	−228.7	(−220.0)	−222.0	−216.9	85.37	87.54
3.4	−129.3	(−123.3)	−128.8	(−122.8)	−130.5	−130.1	(−123.4)	−129.6	(−123.0)	−123.6	−123.7	50.15	51.58
3.6	−72.46	(−67.79)	−72.30	(−67.66)	−71.9	−72.64	(−67.80)	−72.49	(−67.67)	−67.82	−68.83	28.88	29.76
3.8	−40.03	(−36.46)	−39.98	(−36.43)	−38.7	−40.23	(−36.46)	−40.19	(−36.42)	−36.46	−37.31	16.37	16.89
4.0	−21.71	(−19.05)	−21.69	(−19.04)	−20.2	−21.95	(−19.05)	−21.94	(−19.04)	−19.05	−19.58	9.167	9.461
4.4	−5.877	(−4.613)	−5.876	(−4.616)	−4.9	−6.507	(−4.617)	−6.507	(−4.616)	−4.617	−4.764	2.772	2.863
4.8	−1.366	(−0.9118)	−1.366	(−0.9118)	−0.96	−1.852	(−0.9118)	−1.852	(−0.9118)	−0.9120	−0.9420	0.7821	0.8079
5.5	−0.0604	(−0.0295)	−0.0604	(−0.0295)	−0.03	−0.618	(−0.291)	−0.618	(−0.0291)	−0.0295	−0.0305	0.0617	0.0637
6.0	−0.0055	(−0.0014)	−0.0055	(−0.0014)	−0.001	−0.0466	(−0.0013)	−0.0466	(−0.0013)	−0.0016	−0.0016	0.0067	0.0069
10.0	0.00	(0.00)	0.00	(0.00)	−0.00	−0.00	(0.00)	−0.00	(0.00)	−0.00	−0.00	0.00	0.00

a) [||] means a parallel stacking [face-to-face stacking] shown in Figs. 6A and 6B. b) [⊥] means a perpendicular stackin shown in Fig. 6C. c) 6-31G* basis set. d) 4-31G basis set in parenthesis. e) 4-31G basis set.

were explicitly considered to derive Eqs. 2 and 7 for clusters, as illustrated in Fig. 2. Table 1 also summarizes the calculated J_{ab} values for **2** by the UHF/6-31G* method. The magnitude of the J_{ab}(UHF) and J_{ab}(APUHF) values are almost the same, even for the trimer (**2**). The J_{ab} values for **2** are also close to the corresponding J_{ab} values for the dimer (**1**). This supports the nearest-neighbor approximation used in Eqs. 2 and 7. The slight difference on the J_{ab} value between the dimer (**1**) and trimer (**2**) should be related to the weak delocalization effect in the latter.

A linear cluster (**3**) comprising eleven triplet methylenes in face-to-face stacking, as illustrated in Fig. 6B, was examined by the UHF/4-31G method. The total energies of both the LS triplet and HS 23-th multiplet ($S = 11$) states of **3** were calculated with changing the intermolecular distance, R. The calculated J_{ab} values are also given in Table 1. From Table 1, both J_{ab} values by UHF and APUHF are negative in sign, showing an antiferromagnetic spin alignment within the cluster (**3**). The difference between J_{ab}(UHF) and J_{ab}(APUHF) is small, even in **3**, in accord with the small orbital overlaps between the magnetic orbitals in the Region III shown in Fig. 1. The magnitude of the J_{ab} value for the cluster (**3**) is quite similar to the corresponding value for the dimer (**1**) and trimer (**2**), showing a non-dependency of the size effect of clusters. The present numerical results conclude that the sign and magnitude of the J_{ab} values for magnetic clusters comprising triplet methylenes can be estimated on the basis of small cluster models, such as dimer and trimer. Therefore, our previous[5] results for the J_{ab} values calculated from the dimer to pentamer of organic radicals, such as *p*-NPNN, should be applicable to larger clusters as well.

The calculated J_{ab} values for face-to-face clusters of triplet methylenes are negative in sign. The negative J_{ab} values mean that the spins ($S_a = S_b = 1$) at sites a and b align intermolecularly in the antiparallel manner. The orbital average J_{ab} value for the dimer (**1**) is given by

$$J_{ab} = (2 \times 2)^{-1}(J_{p\sigma-p\sigma} + J_{n-n} + 2J_{n-p\sigma}), \tag{14}$$

where $J_{p\sigma-p\sigma}$, Jn-n and $J_{n-p\sigma}$ denote, respectively, the effective exchange integrals for the $p\sigma$–$p\sigma$, n–n (n: lone pair orbital), and n–$p\sigma$ orbital pairs as illustrated in Fig. 7A. Although the sign of $J_{p\sigma-p\sigma}$ and J_{n-n} should be negative (antiferromagnetic) because of non-zero orbital overlaps, the sign of $J_{n-p\sigma}$ becomes positive (ferromagnetic) because of the orbital orthogonality. The negative J_{ab} value implies that the $p\sigma$–$p\sigma$ orbital overlap interaction plays a predominant role for the effective exchange interaction in this conformation, in conformity with our orbital overlap and orientation principles for molecular magnetism.[42]

Similarly, the orbital average J_{ab} value for the dimer in the perpendicular stacking illustrated in Fig. 7B is given by

$$J_{ab} = (2 \times 2)^{-1}(J_{p\sigma-p\pi} + J_{n-p\pi} + J_{p\sigma-n} + J_{n-n}). \tag{15}$$

It is expected from a consideration of the orbital orthogonality and non-zero orbital overlap interaction that the $J_{p\sigma-p\pi}$ and $J_{n-p\pi}$ values should be positive in sign, and $J_{p\sigma-n}$ and J_{n-n}

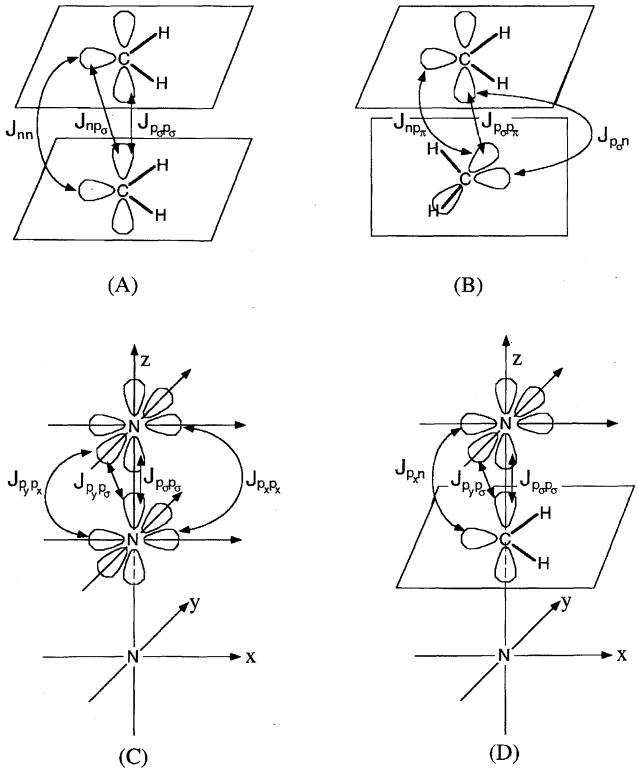

Fig. 7. Schematic representations of the orbital averaged effective exchange integral J_{ab} composed of exchange integrals between interatomic orbitals. (A) $(CH_2)_2$; face-to-face conformation, (B) $(CH_2)_2$; perpendicular conformation, (C) dimer composed of quartet nitrogen atoms, (D) dimer composed of quartet nitrogen atom and triplet methylene

are negative. It can be seen from Table 1 that the calculated J_{ab} value for a cluster (**4**) of eleven triplet methylene in the perpendicular stacking shown in Fig. 1C are positive in sign in all of the interatomic regions examined here. This indicates that the orbital orthogonality effects of p_σ–p_π n–p_π are more important for the effective exchange integral in **4** than the orbital overlap interaction of p_σ–n and n–n, in contrast with the case of the face-to-face comformers (**1**—**3**).

The UNO CAS for **3** and **4** is twenty two active orbitals and twenty two active electrons {22,22}. The J_{ab} values for **3** and **4** by APUHF should be close to those of CASCI{22, 22} and CASSCF{22,22}.

2. 2. Linear Cluster of Quartet Nitrogen Atoms. The ground state of the nitrogen atom is a quartet and the orbital average J_{ab} value for the dimer (**5**) of the quartet nitrogen atom is given by, as illustrated in Fig. 7C,

$$J_{ab} = (3 \times 3)^{-1}(J_{p\sigma-p\sigma} + 2J_{px-px} + 4J_{p\sigma-py} + 2J_{px-py}), \quad (16)$$

where J_{px-px}, $J_{p\sigma-py}$, and J_{px-py} denote, respectively, the effective exchange integrals for the p_x–p_x, p_σ–p_y, and p_x–p_y orbital pairs. The sign of $J_{p\sigma-p\sigma}$ and J_{px-px} should be negative (antiferromagnetic) because of non-zero orbital overlaps, but the sign of $J_{p\sigma-py}$ and J_{px-py} becomes positive (ferromagnetic) because of the orbital orthogonality. Since the p_σ–p_σ orbital overlap interaction plays a predominant role for the effective exchange interaction in **5**, the J_{ab} value for **5** should be negative, but its magnitude becomes smaller than that of the triplet methylene dimer, since the latter two terms in Eq. 16 are contributable.

In order to confirm the above prediction, a linear cluster (**6**) comprising eleven nitrogen atoms with equal interatomic distance was examined by the UHF/4-31G method. Both the LS quartet and HS ($S = 33/2$) states were constructed, and the total energies of these states were calculated to obtain a J_{ab} value for **6** using Eq. 2. They are summarized in Table 2. The J_{ab} values for **6** are negative in the region 3.0 Å$<R<$10 Å, showing that the antiferromagnetic spin alignment is more stable than other spin alignments, such as the ferromagnetic one. The J_{ab} values by UHF and APUHF were calculated to be quite similar, in conformity with the small orbital overlaps between the magnetic orbitals in **6**. The magnitude of the J_{ab} value was reduced to about one-tenth of the J_{ab} value of the methylene cluster (**3**), supporting the above orbital interaction arguments based on the model in Fig. 7.

The UNO CAS space for **6** becomes thirty three active orbitals and thirty three active electrons {33,33} CASCI and CASSCF calculations using this large space are impossible at the percent stage. On the other hand, the present and previous results[5,6] show that the approximate spin-projected UHF (APUHF) procedure can be used to estimate the effective exchange integrals, even for large clusters of organic radicals, such as triplet methylene and quartet nitrogen atom. It can be used as a practical technique when the UNO CASCI and UNO CASSCF calculations are impossible because of too many active orbitals.

2. 3. Linear Cluster of Six Quartet Nitrogen Atoms Plus Five Triplet Methylenes. Figure 6D shows a linear cluster (**7**) comprising five triplet methylenes and six quartet nitrogen atoms. This cluster has a distinct size of spins, such as $S_a = 3/2$ and $S_b = 1$, at sites a and b for nitrogen atoms and methylenes, respectively, being different from those having an equivalent size of spins of $S_a = S_b = 1$ in the case of linear clusters comprising triplet methylenes. The orbital average J_{ab} value for the dimer of the nitrogen atom and methylene, which is illustrated in Fig. 7D, is given as

Table 2. Effective Exchange Integrals J_{ab} (cm^{-1}) of Linear Clusters of N_{11} and N–$(CH_2$–N$)_5$ Using 4-31G Basis Set

R	N_{11}		N–$(CH_2$–N$)_5$	
Å	UHF	APUHF	UHF	APUHF
3.0	−31.77	−31.96	−120.0	−117.3
3.2	−15.82	−15.82	−64.31	−64.06
3.4	−7.896	−7.919	−34.17	−34.41
3.6	−3.913	−3.930	−17.90	−18.13
3.8	−1.891	−1.901	−9.152	−9.302
4.0	−0.8737	−0.8786	−4.519	−4.601
4.4	−0.1533	−0.1542	−0.9490	−0.9674
4.8	−0.0195	−0.0197	−0.1547	−0.1577
5.5	−0.0023	−0.0024	−0.0031	−0.0032
6.0	−0.0000	−0.0000	−0.0001	−0.0001
10.0	0.0000	0.0000	0.0000	0.0000

$$J_{ab} = (3 \times 2)^{-1}(J_{px-n} + J_{py-n} + J_{p\sigma-n} + J_{py-p\sigma} + J_{px-p\sigma} + J_{p\sigma-p\sigma}), \quad (17)$$

where J_{px-n}, $J_{p\sigma-n}$, and $J_{p\sigma-p\sigma}$ values should be negative in sign because of a non-zero orbital overlap, which the J_{py-n}, $J_{py-p\sigma}$, and $J_{px-p\sigma}$ values becomes positive in sign due to the orbital orthogonality. The effective exchange integrals (J_{ab}) at the levels of UHF/4-31G and APUHF/4-31G are also summarized in Table 2. The J_{ab} values are negative in sign for both methods in the region 3.0 Å$<R<$10.0 Å examined here, indicating that an antiparallel spin alignment (antiferromagnetic) is more stable than a parallel spin alignment (ferromagnetic). The negativity of the J_{ab} values comes from greater contributions of J_{px-n}, $J_{p\sigma-n}$, and $J_{p\sigma-p\sigma}$ rather than J_{py-n}, $J_{py-p\sigma}$, and $J_{px-p\sigma}$. $J_{p\sigma-p\sigma}$ could be expected to be the main factor because of a strong $p\sigma$–$p\sigma$ overlap. It is, furthermore, noted that the APUHF method gives J_{ab} values similar to those of UHF method, even different sizes of spins at sites a and b, compared with the cases of equivalent sizes of spins at sites a and b.

The UNO CAS space for **7** is twenty eight active orbitals and twenty eight active electrons {28,28}. Judging from the computational results given in Table 1, the APUHF would be a good approximation to UNO CASSCF {28,28},[6] which is impossible for this ferrimagnetic cluster (**7**) at the present stage.

3. Dynamical Correlation Corrections for J_{ab} Value

3. 1. Comparison Among Several Post Hartree–Fock and Density Functional Methods. Dynamical correlation corrections are usually essential for the Hartree–Fock solution and even for the UNO CASCI and CASSCF solutions to depict reliable potential curves for organic reactions.[7,35,36] The situation should be similar to the computations of the J_{ab} values for organic radical clusters. It is, therefore, important and instructive to discuss here the correlation correction for J_{ab}. We previously carried out several post Hartree–Fock calculations; namely, UHF Möller–Plesset perturbation (UMP) and coupled-cluster (UCC) calculations followed by the approximate spin-projection (AP), as shown in Eqs. 7, 8, and 9.[6] Second-order configuration interaction (SOCI) and multireference single and double CI (MRSDCI) calculations were also examined in order to obtain the J_{ab} values for the triplet methylene dimer (**1**).[6] In addition, we previously performed second-order perturbation calculations based on the CASSCF solution[27] in order to compare with the variational CI and perturbation method:[6] namely, the CASPT2[31] and MRMP2[43,44] computations of the J_{ab} values for **1**. We summarize the previously calculated results in Table 3. From Table 3, we can make the following conclusions:

(1) The J_{ab} values by the APUMP2 and APUCCSD methods are negative over the entire region examined here. The sign of J_{ab} does not change after dynamical correlation corrections for the UHF results by the MP2 and CCSD methods.

(2) The J_{ab} values by the SOCI method are negative over the entire region examined here. However, the sign of the J_{ab} value by MRSDCI changes from negative to positive near to the intermolecular distance $R = 4.5$ Å, showing a spin crossover from the LS state to the HS state.

(3) The J_{ab} values by CASPT2(D)[27] are negative over the entire region like the SOCI. However, the sign of the J_{ab} value by MRMP2 changes near $R = 5.5$ Å, showing a spin crossover, as in the case of MRSDCI.

From the above results, well-balanced descriptions between the LS and HS states are necessary to obtain reasonable J_{ab} value. The MRSDCI and MRMP2[6] methods should be carefully used for computations of very small J_{ab} values, since the MRSDCI and MRMP2 methods suffer from a size-inconsistency error in the dissociation region. In other words, the SOCI method should involve well-balanced configuration of much more triple, quadruple, and other higher excitations, which are responsible for the product term of single and double excitations of fragments, such as triplet methylene. The UMP2 followed by an approximate spin projection (AP), APUMP2, can be used as an effective alternative to SOCI or CASPT2 for larger clusters of organic radicals.

The density functional (DFT) methods have been successfully applied to computations of the potential surfaces

Table 3. Effective Exchange Integrals J_{ab} (cm^{-1}) of Face-to-Face Dimer of Triplet Methylene with Effects of Electronic Correlations Using 6-31G* Basis Set
There values are referred to Refs. 6a and 6b.

R	post UHF		CI		CASMP	
(Å)	APUMP2	APUCCSD	SOCI	MRSDCI	CASPT2(D)	MRMP2
3.0	−463.1	−494.8	−466.6	−460.1	−492.6	−496.1
3.2	−266.4	−279.0	−266.3	−260.8	−283.6	−283.7
3.4	−152.1	−157.2	−150.0	−145.0	−161.7	−162.7
3.6	−85.96	−88.10	−82.9	−78.2	−91.18	−91.49
3.8	−47.86	−48.76	−44.7	−40.2	−50.61	−50.60
4.0	−26.11	−26.48	−23.4	−19.0	−27.51	−27.34
4.4	−7.126	−7.175	−5.65	−1.4	−7.450	−7.198
4.8	−1.652	−1.652	−1.13	3.2	−1.719	−1.498
5.5	−0.0768	−0.0768	−0.037	3.2	−0.0830	0.0638
6.0	−0.0055	−0.0110	0.0	4.0	−0.0073	0.0971
10.0	0.0000	0.0000	0.0	4.2	0.0	0.6399

organic reactions. Therefore, it is particularly interesting to examine the applicabilities of the DFT methods to compute the J_{ab} values for the triplet methylene dimer (**1**). The spin-projection scheme by Eq. 2 is equally applicable to the DFT method, since it utilizes the expectation values of the total spin angular momentums. Table 4 summarizes the calculated results. From Table 4, the following conclusions are drawn:

(4) The J_{ab} values by BLYP are negative over the entire region. However, the magnitude of the J_{ab}(AP-BLYP) is several times larger than those of APUMP2 and CASPT2 in the region; 3.0 Å$<R<$4.8 Å. The stability of the LS state is relatively overestimated by BYLP.

(5) The $|J_{ab}|$ values by B3LYP are smaller than those of BLYP, showing a significant improvement in the overstabilization of the LS state by BLYP. However, the magnitude of J_{ab}(B3LYP) is still larger than those of APUMP2 and CASPT2 over the entire region. From Tables 3 and 4, the B3LYP method is seen to be applicable for qualitative discussions of J_{ab} values for organic radical clusters.[6] It is, however, noteworthy that the DFT method often overestimates stability of the low-spin state for a radical cluster.[45]

Table 4. Effective Exchange Integrals J_{ab} (cm^{-1}) of Face-to-Face Dimer of Triplet Methylene at Level of DFT/6-31G*

R	BLYP		B3YLP	
Å	BLYP	APBLYP	B3LYP	APB3LYP
3.0	−1060.7	−981.1	−826.1	−790.1
3.2	−655.0	−623.5	−502.1	−488.6
3.4	−404.2	−392.1	−305.5	−300.6
3.6	−247.4	−242.9	−184.6	−182.9
3.8	−149.8	−148.3	−110.7	−110.1
4.0	−88.80	−88.26	−65.02	−64.83
4.4	−28.97	−28.87	−20.95	−20.93
4.8	−8.552	−8.535	−6.144	−6.143
5.5	−0.8049	−0.8049	−0.5765	−0.5765
6.0	−0.1341	−0.1333	−0.0961	−0.0961
10.0	0.0000	−0.0000	0.0001	−0.0000

3. 2. APUMP2 Calculations of Clusters with Eleven Magnetic Sites. The preceding results demonstrate that the dynamical correlation corrections are crucial for quantitative discussions of the J_{ab} values for radical clusters. For example, the $|J_{ab}|$ value for the triplet methylene dimer (**1**) at R = 3.0 Å by the Hartree–Fock mean-field approximation increases by 17 and 25% after correlations by MP2 and CCSD, respectively. Similarly, the $|J_{ab}|$ value by CASSCF increases by 20 and 21% after dynamical correlations by CASPT2 and MRMP2, respectively. However, the sign of the J_{ab} value for **1** in the large R region becomes incorrect when using the MRSDCI and MRMP2 methods after these correlation corrections. Therefore, it is interesting to examine the reliability of the APUMP2 method for clusters with eleven magnetic sites. We examined clusters comprising eleven triplet methylenes in the face-to-face (parallel) and perpendicular stackings, as shown in Figs. 7B and 7C, together with a mixed column with five triplet methylenes and six nitrogen atoms in Fig. 7D. The J_{ab} values calculated for these three clusters by UMP2/4-31G are summarized in Table 5.

From Table 5, the signs of the J_{ab} values of all the clusters are kept in all of regions examined here, showing that the spin crossovers do not occur between the LS and HS states. The J_{ab} values of a face-to-face cluster of eleven triplet methylene, estimated by APUMP2 method, are slightly smaller than those of dimer (in Table 3) because of different basis sets, such as 6-31G* and 4-31G, in harmony with the tendency between the UHF and APUHF methods for the cluster of triplet methylene shown in Table 1. The $|J_{ab}|$ values of $(CH_2)_{11}$ in the face-to-face stacking and N–$(CH_2$–N$)_5$ by UMP2 and APUMP2 are larger than those by the UHF and APUHF methods, respectively, being similar to the case of the dimer of triplet methylenes under correlation corrections. On the contrary, the J_{ab} values of $(CH_2)_{11}$ in perpendicular stacking at the levels of UMP2 and APUMP2 are much smaller than those at the UHF levels. This implies that the LS state is much more stabilized by the dynamical correlation correction than the HS state in this conformation.

Table 5. Effective Exchange Integrals J_{ab} (cm^{-1}) of Linear Clusters Estimated at Level of MP2/4-31G

R	$(CH_2)_{11}$[‖][a]		$(CH_2)_{11}$[⊥][b]		N–$(CH_2$–N$)_5$[c]	
Å	UMP2	APUMP2	UMP2	APUMP2	UMP2	APUMP2
3.0	−467.7	−423.2	127.4	128.8	−144.9	−138.5
3.2	−263.9	−250.0	78.17	79.17	−78.19	−76.50
3.4	−147.6	−144.0	46.77	47.39	−41.78	−41.42
3.6	−81.45	−80.80	27.46	27.84	−21.96	−21.93
3.8	−43.96	−44.06	15.89	16.11	−11.25	−11.28
4.0	−23.02	−23.20	9.084	9.209	−5.546	−5.576
4.4	−5.580	−5.650	2.856	2.895	−1.158	−1.166
4.8	−1.098	−1.113	0.8287	0.8402	−0.1873	−0.1886
5.5	−0.0352	−0.0356	0.0667	0.0676	−0.0039	−0.0039
6.0	−0.0018	−0.0019	0.0075	0.0076	−0.0001	−0.0001
10.0	−0.0000	−0.0000	0.0000	0.0000	0.0000	0.0000

a) Face-to-face stacking shown in Fig. 6B. b) Perpendicular stacking shown in Fig. 6C.
c) Linear stacking shown in Fig. 6D.

Table 6. Effective Exchange Integrals J_{ab} (cm^{-1}) of Linear Clusters Estimated at Level of B3LYP/4-31G

R	$(CH_2)_{11}[\|\|]$[a]		$(CH_2)_{11}[\perp]$[b]		N_{11}		$N–(CH_2–N)_5$[c]	
Å	B3LYP	APB3LYP	B3LYP	APB3LYP	B3LYP	APB3LYP	B3LYP	APB3LYP
3.0	−792.7	−590.8	56.35	55.19	−93.93	−89.73	−307.7	−260.0
3.2	−478.7	−396.6	38.95	38.71	−52.38	−51.18	−182.5	−164.7
3.4	−287.6	−256.9	25.52	25.55	−29.23	−28.93	−106.9	−100.8
3.6	−202.3	−189.9	16.37	16.44	−15.89	−15.83	−61.41	−59.58
3.8	−99.25	−96.18	10.45	10.52	−8.471	−8.468	−34.16	−33.71
4.0	−55.98	−55.29	6.699	6.750	−4.342	−4.348	−18.43	−18.36
4.4	−16.09	−16.16	2.718	2.742	−1.107	−1.110	−4.509	−4.528
4.8	−4.143	−4.177	0.9939	1.003	−0.1687	−0.1692	−0.8994	−0.9049
5.5	−0.3106	−0.3134	0.1152	0.1162	−0.0126	−0.0126	−0.0375	−0.0378
6.0	−0.0460	−0.0464	0.0208	0.0210	−0.0001	−0.0001	−0.0074	−0.0074
10.0	−0.0006	−0.0006	0.0000	0.0000	0.0000	0.0000	0.0000	0.0000

a) Face-to-face stacking shown in Fig. 6B. b) Perpendicular stacking shown in Fig. 6C. c) Linear stacking shown in Fig. 6D.

3. 3. DFT Calculations of Clusters with Eleven Magnetic Sites. The utility and applicability of the density functional method were also investigated for linear radical clusters comprising eleven triplet methylenes, eleven quartet nitrogen atoms, and five triplet methylenes plus six quartet nitrogen atoms at the B3LYP/4-31G level. The calculated J_{ab} values are summarized in Table 6, giving the following results:

(1) The $|J_{ab}|$ values of $(CH_2)_{11}$ by B3LYP are larger than those of APB3LYP in the small intermolecular region (R<3.5 Å) for face-to-face stacking, showing a significant orbital-overlap effect under the DFT approximation.

(2) The $|J_{ab}|$ values of $(CH_2)_{11}$ in face-to-face stacking at the level of APB3LYP/4-31G are larger than those at the APUMP2/4-31G level with the correlation corrections shown in Table 5. Similarly, the $|J_{ab}|$ values of $N–(CH_2–N)_5$ are still larger than those of APUMP2.

(3) The $|J_{ab}|$ value of N_{11} are several times larger than those of APUHF shown in Table 2.

(4) The J_{ab} values of $(CH_2)_{11}$ in the perpendicular stacking at the level of APB3LYP/4-31G are surprisingly smaller than those by APUMP2.

(5) The density functional methods have tendencies to emphasize the negativity (antiferromagnetic character) and to suppress the positivity (ferromagnetic character) of the effective exchange integrals for the linear radical clusters examined here.

Based on Tables 5 and 6, the B3LYP method is seen to be applicable for qualitative discussions of the J_{ab} values for organic radical clusters, even with long linear stacking. It is, however, noteworthy that the DFT method often overestimates the stability of the low-spin state and the contribution from the exchange integrals of non-zero orbital overlap for radical clusters. Therefore, it predicted a negative (antiferromagnetic) J_{ab} value for a hydrogen-bridged system, though the experiment showed a positive (ferromagnetic) J_{ab} value.[45]

4. Concluding Remarks

In this paper both spin-restricted and unrestricted ab initio calculations of effective exchange integrals were carried out for dimer, trimer, and clusters with eleven magnetic sites, where triplet methylene and quartet nitrogen atoms were used as the magnetic components. As a spin-restricted approach, the CASSCF calculations were first carried out for the dimer of triplet methylene, followed by the SO-CI, MRSDCI, CASPT2(D), and MRMP2 calculations for dynamical correlation corrections. It was found that all of the post CASSCF methods provide similar J_{ab} values in the intermediate region, where the intermolecular distance (R) is variable from 3 to 4 Å. However, the MRSDCI and MRMP2 showed a spin crossover from the low-spin (LS) state to high-spin (HS) state at R = 4.5 Å and at R = 5.5 Å, respectively. This implies that well-balanced computations of both the LS and HS states are crucial, even in the spin-restricted approaches. On the other hand, the MP2 and CCSD(T) methods based on the UHF solutions provided similar J_{ab} values to those of SO-CI and CASPT2 if a size-consistent spin projection is performed, as discussed here.

In changing the cluster size of the triplet methylene from 2 and 3 to 11, J_{ab}(APUMP2)-values remains reasonably constant, showing that the approximate projected UMP2 (APUMP2) method has merit in that it can be applicable to large magnetic clusters. In fact, APUMP2 was successfully applied to magnetic clusters with eleven magnetic sites. The APUMP2 calculations of ten to one-hundred hydrogen clusters (H_{10}—H_{100})[5] were already carried out to elucidate ten potential curves and J_{ab} values in mesoscopic clusters. The potential curves before and after a size-consistent spin projection were almost the same for the H_{100} magnetic cluster, supporting Eqs. 8, 9, 10, 11, and 12 and Fig. 4.

The hybrid method (B3LYP) provided reasonable J_{ab} values for the organic radical clusters examined here, being a useful hand for qualitative purposes, though it is still insufficient for quantitative purposes, because of a general overstabilization of the low-spin (LS) state. The more reliable hybrid procedures in the DFT formalism to reproduce the SO-CI and CASPT2 results[6] are desirable for quantitative discussions of molecular magnetism.[1]

Recently, nanoscale magnetic clusters have been synthesized by several groups.[46] These are indeed receiving current interest in relation to opportunities of new chemical physics,

such as superparamagnetism, macroscopic quantum tunneling (MQT), single molecular magnet and active controls of molecular magnetism by the external fields.[47] Carbene and nitrene groups as well as many other radicals have been used as building blocks for mesoscopic organic magnetic clusters, though chemical reactivities of radical sites should be suppressed by appropriate procedures. To avoid such instabilities of spin sources in molecular magnets, hybrid systems comprising organic spin couplers and spins of transition metal ions would be the next synthetic targets in this field. Both experimental and theoretical efforts[39] are desirable. The UMP2 and B3LYP methods, followed by size-consistent spin projection, will be hopefully used for the molecular design of such new dπ–pπ conjugated systems.

This work was supported by Grants-in-Aid for Scientific Research on Priority Areas (No. 283, " Innovative Synthetic Reactions" and No. 282, "Electrochemistry of Ordered Interface") from the Ministry of Education, Science, Sports and Culture.

References

1) a) J. S. Miller and D. A. Dougherty, *Mol. Cryst. Liq. Cryst.*, **176**, (1989); b) D. Gatteschi, O. Kahn, J. S. Miller, and F. Palacio, "Mabnetic Molecular Materials," NATO ASI Series No. 198, Kluwer Academic Pub., (1991); c) H. Iwamura and J. S. Miller, *Mol. Cryst. Liq. Cryst.*, **232** and **233**, (1992); d) J. S. Miller et al., *Mol. Cryst. Liq. Cryst.*, **271**, (1995).

2) J. G. Bednorz and K. A. Muller, *Z. Phys. B*, **B64**, 189 (1986).

3) a) K. Yamaguchi, Y. Takahara, T. Fueno, K. Nakasuji, and I. Murata, *Jpn. J. Appl. Phys.*, **27**, L766 (1988); b) K. Yamaguchi, H. Namimoto, T. Fueno, T. Nogami, and Y. Shirota, *Chem. Phys. Lett.*, **166**, 408 (1990); c) K. Yamaguchi, M. Okumura, T. Fueno, and K. Nakasuji, *Synth. Metals*, **41—43**, 3631 (1991).

4) a) J. R. Hart, A. K. Rappe, S. M. Gorun, and T. H. Upton, *J. Phys. Chem.*, **96**, 6264 (1992); b) K. Fink, R. Fink, and V. Staemmler, *Inorg. Chem.*, **33**, 6219 (1994); c) O. Catell, R. Caballol, V. M. Garcia, and K. Handrick, *Inorg. Chem.*, **35**, 1609 (1996).

5) a) K. Yamaguchi, M. Okumura, J. Maki, T. Noro, H. Namimoto, M. Nakano, T. Fueno, and K. Nakasuji, *Chem. Phys. Lett.*, **190**, 353 (1992); b) M. Okumura, K. Yamaguchi, M. Nakano, and W. Mori, *Chem. Phys. Lett.*, **207**, 1 (1993); c) K. Yamaguchi, M. Okumura, S. Yamanaka, T. Kawakami, Y. Yoshioka, T. Noro, and F. Sasaki, to be published (detail derivations of Eq. 6 were performed).

6) a) K. Yamaguchi, M. Okumura, W. Mori, J. Maki, K. Takada, T. Noro, and K. Tanaka, *Chem. Phys. Lett.*, **210**, 201 (1993); b) S. Yamanaka, M. Okumura, K. Yamaguchi, and K. Hirao, *Chem. Phys. Lett.*, **225**, 213 (1994); c) S. Yamanaka, T. Kawakami, H. Nagao, and K. Yamaguchi, *Chem. Phys. Lett.*, **231**, 25 (1994).

7) Y. Yoshioka, D. Yamaki, G. Maruta, T. Tsunesada, K. Takada, T. Noro, and K. Yamaguchi, *Bull. Chem. Soc. Jpn.*, **69**, 3395 (1996).

8) C. C. J. Roothaan, *Rev. Mod. Phys.*, **23**, 69 (1951).

9) W. J. Hehre, L. Radom, P. v. R. Schleyer, and J. A. Pople, "Ab initio Molecular Orbital Theory," Wiley, New York (1986).

10) a) K. Yamaguchi, *Chem. Phys. Lett.*, **33**, 330 (1975); b) K. Yamaguchi, *Chem. Phys. Lett.*, **35**, 230 (1975).

11) D. J. Thouless, "The Quantum Mechanics of Many-Body Systems," Academic Press, New York (1961).

12) J. Cizek and J. Paldus, *J. Chem. Phys.*, **47**, 3976 (1967).

13) H. Fukutome, *Prog. Theoret. Phys.*, **47**, 1156 (1972).

14) K. Yamaguchi, T. Fueno, and H. Fukutome, *Chem. Phys. Lett.*, **22**, 466 (1973).

15) K. Yamaguchi, Y. Takahara, T. Fueno, and K. N. Houk, *Theoret. Chim. Acta*, **73**, 337 (1988).

16) K. Yamaguchi, Y. Takahara, and T. Fueno, "Appl. Quant. Chem.," ed by V. H. Smith, H. F. Schaefer, III, and K. Morokuma, D. Reidel Pub. Co., Boston (1986), p. 155.

17) H. B. Schlegel, *J. Chem. Phys.*, **84**, 4530 (1986).

18) P. J. Knowles and N. C. Handy, *J. Chem. Phys.*, **88**, 6991 (1988).

19) C. Möller and M. S. Plesset, *Phys. Rev.*, **46**, 618 (1934).

20) J. A. Pople, M. Head-Gordon, and K. Raphavachan, *J. Chem. Phys.*, **87**, 5968 (1987).

21) P. O. Löwdin, *Phys. Rev.*, **97**, 1509 (1955).

22) "Gaussian 92, Revision G. 3," ed by M. J. Frish, G. W. Trucks, M. Head-Gordon, P. M. W. Gill, M. W. Wong, J. B. Foresman, H. B. Schlegel, M. A. Robb, E. S. Replogle, R. Gomperts, J. L. Andres, K. Raghavachari, J. S. Binkley, C. Gonzalez, R. L. Martin, D. J. Fox, D. J. Defrees, J. Baker, J. J. P. Stewart, and J. A. Pople, Gaussian, Inc, Pittsburgh, PA (1992).

23) A. T. Amos and G. G. Hall, *Proc. R. Soc. London, Ser. A*, **A263**, 483 (1961).

24) K. Yamaguchi, K. Ohta, S. Yabushita, and T. Fueno, *Chem. Phys. Lett.*, **49**, 555 (1977).

25) a) K. Yamaguchi, *Int. J. Quantum Chem., Symp.*, **14**, 269 (1980); b) S. Yamamoto, K. Yamaguchi, and K. Nasu, *Phys. Rev. B*, **42**, 265 (1990).

26) K. Rudenberg, L. M. Cheung, and S. T. Elbert, *Int. J. Quantum Chem.*, **16**, 1069 (1979).

27) B. Roos, *Int. J. Quantum Chem., Symp.*, **14**, 175 (1980).

28) P. Pulay and T. P. Hamilton, *J. Chem. Phys.*, **88**, 4926 (1988).

29) J. M. Bofill and P. Pulay, *J. Chem. Phys.*, **90**, 3657 (1989).

30) K. Wolinski and P. Pulay, *J. Chem. Phys.*, **90**, 36497 (1989).

31) K. Andersson, Per-A. Malmquist, and B. O. Roos, *J. Chem. Phys.*, **96**, 1218 (1992).

32) K. Yamaguchi, Y. Toyoda, and T. Fueno, *Chem. Phys. Lett.*, **159**, 459 (1989).

33) K. Yamaguchi, H. Fukui, and T. Fueno, *Chem. Lett.*, **1986**, 625.

34) K. Yamaguchi, H. Namimoto, and T. Fueno, *Mol. Cryst. Liq. Cryst.*, **176**, 151 (1989).

35) a) K. Yamaguchi, F. Jensen, A. Dorigo, and K. N. Houk, *Chem. Phys. Lett.*, **149**, 537 (1988); b) Y. Takahara, K. Yamaguchi, and T. Fueno, *Chem. Phys. Lett.*, **158**, 95 (1989).

36) S. Yamanaka, M. Okumura, M. Nakano, and K. Yamaguchi, *J. Mol. Struct. (Theochem.)*, **310**, 225 (1994).

37) Y. Yoshioka, S. Kubo, S. Kiribayashi, Y. Takano, and K. Yamaguchi, *Bull. Chem. Soc. Jpn.*, **71**, 573 (1998).

38) K. Yamaguchi, T. Kawakami, D. Yamaki, and Y. Yoshioka, "Molecular Magnetism," ed by K. Ito, Kodansha Scientific, Tokyo (1998), in press.

39) M. Nishino, S. Yamanaka, Y. Yoshioka, and K. Yamaguchi, *J. Phys. Chem. A*, **101**, 705 (1997).

40) M. Nishino, Y. Yoshioka, K. Yamaguchi, K. Mashima, K. Tani, and A. Nakamura, *Bull. Chem. Soc. Jpn.*, **71**, 99 (1998).

41) a) K. Yamaguchi, T. Fueno, N. Ueyama, A. Nakamura, and M. Ozaki, *Chem. Phys. Lett.*, **164**, 210 (1989); b) K. Yamaguchi, T. Fueno, M. Ozaki, N. Ueyama, and A. Nakamura, *Chem. Phys. Lett.*, **164**, 210 (1989).

42) T. Kawakami, S. Yamanaka, W. Mori, K. Yamaguchi, A. Kajiwara, and M. Kamachi, *Chem. Phys. Lett.*, **235**, 414 (1995).
43) K. Hirao, *Chem. Phys. Lett.*, **196**, 403 (1992).
44) H. Nakano, *J. Chem. Phys.*, **99**, 7983 (1993).
45) T. Kawakami, S. Takeda, W. Mori, and K. Yamaguchi, *Chem. Phys. Lett.*, **261**, 129 (1996).
46) D. Gatteschi, A. Caneschi, L. Pardi, and R. Sessoli, *Science*, **265**, 1054 (1994).
47) D. Gatteschi and K. Yamaguchi, "Molecular Magnetism: from Molecular Assemblies to the Devices," ed by E. Coronado, Kluwer Academic Pub., (1996), pp. 561—570.